Effects of the Formation of Copolymer on the Interfacial Adhesion between Semicrystalline Polymers

Eric Boucher, John P. Folkers, Hubert Hervet, and Liliane Léger*

Laboratoire de Physique de la Matière Condensée,† Collège de France, 11 place Marcelin Berthelot, 75231 Paris Cedex 05, France

Costantino Creton

Laboratoire de Physico-chimie Structurale et Macromoléculaire, ESPCI, 10 rue Vauquelin, 75231 Paris Cedex 05, France

Received July 3, 1995; Revised Manuscript Received October 2, 1995⊗

ABSTRACT: The relationship between the fracture toughness (G_c) and the areal density of diblock copolymer at the interface (Σ) was investigated for joints between polypropylene (PP) and polyamide-6 (PA6), two incompatible, semicrystalline polymers. Diblock copolymers were formed *in situ* by reaction between succinic acid groups terminally grafted onto 5% of the PP chains and the NH_2 ends of the PA6 chains. Fracture toughnesses were measured using an asymmetric double cantilever beam test (ADCB). After the bulk PA6 had been completely rinsed from an adhered sample, X-ray photoelectron spectroscopy (XPS) was used to measure the areal density of copolymer at the interface. Above the melt temperature of PP, but below that of PA6, reaction at the interface was limited by diffusion of the reactive PP chains ($D = 1.58 \times 10^{-11}$ cm^2 s^{-1} at 213 °C). By controlling the temperature and the time of formation, G_c could be varied in the range from 5 to 100 J/m^2. Dissipation during fracture was observed to occur by plastic deformation in the PP, and failure of the joint was determined to occur by chain scission of the PP part of the copolymer. The fracture toughness was found to vary as the square of the areal density of copolymer at the interface, a relationship similar to that observed and predicted for glassy polymers. This scaling behavior suggests that the stresses in the fracture are concentrated over a distance on the order of 10 nm at the head of the crack.

I. Introduction

Because of improvements in their mechanical and physicochemical properties over those of single-component systems, blends containing two polymers have been used in many important applications. The difficulty in designing such materials is that, in general, the different polymers are immiscible. Their biphasic mixtures consequently have weak interfaces, which result in poor mechanical properties. To increase the mechanical performance of a blend, a third component, or "compatibilizer", is often added. This additive increases the interfacial strength and generally leads to better overall properties. In addition to the industrial interest in compatibilizers, their properties and mechanisms of action have been studied in the academic community, because of their relevance to the general behavior of polymers at interfaces.

A common, effective way of diminishing incompatibility at a polymer/polymer interface is by the addition of copolymer,[1] often a diblock copolymer—that is, a polymer composed of two parts—in which each block is miscible with one of the two homopolymers. The interfacial tension between the two homopolymers is decreased through the decreased chain stretching of the block copolymers when increasing the interfacial area.[2] Dynamic dissipation during separation can also occur, because viscous friction and plastic deformation are spread out over the entire length of the chains and even into the surrounding bulk. Recently, the use of random copolymers was shown to increase the efficiency of dissipation over that of diblock copolymers, by making multiple "excursions" across the interface.[3]

The mechanisms by which copolymers work as compatibilizers have been largely studied for glassy polymers (for a general summary, see ref 4). In the case of diblock copolymers, several mechanisms are possible as a function of their length and of their areal density at the interface. If the degree of polymerization N of one of the blocks is smaller than its average degree of polymerization between entanglements N_e, it will be easily pulled out, leading to relatively weak energies of adhesion ($G_c = 1-6$ J/m^2). In this regime, G_c increases linearly with the areal density of copolymer at the interface (Σ) and varies as the square of the extracted length (i.e., $G_c \sim \Sigma N^2$).[5,6] Near N_e, the diblock can still be pulled out at low densities, but as the areal density is increased, the stress at the interface can reach the critical value for the formation of crazes in one of the materials, which leads to increased dissipation due to collective movements propagated across much larger distances.[7] Significantly above N_e but at low values of Σ, the frictional force on the extracted chain can become too large, leading to scission of the connector chains. As Σ is increased,[6,8] the stress at the interface will again induce the formation of crazes. For some systems in the crazing regime, G_c was found to vary as Σ^2, an effect that has been attributed to a concentration of stresses in the fibrils near the head of the fracture.[7] The transitions between the different regimes outlined above depend on a balance between the force needed to rupture a chemical bond and the force needed to overcome the friction on the monomers.[5,6] An understanding of these various effects for a given system can be used to optimize the reinforcement of an interface between glassy polymers.

Since it is not obvious, *a priori*, that the formalism outlined above for glassy polymers will be applicable when crystallites are present in the polymers, we have examined the effects of copolymer on the reinforcement

† U.R.A. C.N.R.S. 792.

⊗ Abstract published in *Advance ACS Abstracts,* November 15, 1995.

0024-9297/96/2229-0774$12.00/0

Table 1. Molecular Characteristics and Properties of Polymeric Materials

material	M_n	M_w	E,[a] GPa	σ_y,[b] MPa	enthalpy of fusion,[c] J/g
PP	57 000	275 000	—	—	—
PP_s	23 000	61 000	—	—	—
PP*	—[d]	—	1.0 ± 0.13	27	90 ± 5
PA6	17 000	34 000	2.2 ± 0.34	65	70 ± 5

[a] Measured by three-point bending test. [b] Measured at a strain rate of 10^{-4} s^{-1}. [c] Measured using differential scanning calorimetry (Perkin-Elmer DSC 7) at a heating rate of 5 °C/min. [d] A dash means that the measurement was not made.

of the interface between polypropylene (PP) and polyamide-6 (PA6), two semicrystalline polymers. In the present study, we have used samples formed under similar conditions, so as to limit the variation in crystallinity. This system will eventually provide a good system for investigating the role of crystallites on adhesion. Furthermore, it is a good model system with which to investigate more quantitatively the *in situ* formation of block copolymers at interfaces. This methodology for obtaining compatibilizers is widely used in polymeric blends,[9] because in practical cases the formation of micelles often prevents block copolymers from migrating to the interface in reasonable times.

We focus here on the relationship between the energy of adhesion and the areal density of copolymer at the interface. It was therefore necessary to have reliable, reproducible methods for determining both G_c and Σ. The asymmetric double cantilever beam (ADCB) test satisfied the criteria needed to determine G_c. Measurement of Σ was, however, more difficult, because the techniques that have been used for glassy polymers[6,8] cannot be employed for semicrystalline polymers for two main reasons. First, rapid crystallization precludes spin casting of a homogeneous layer of known thickness (and therefore of known density) of either PP or PA6. The copolymer, therefore, had to be placed at the interface by another method, such as *in situ* formation. Second, deuterated polymers could not be used to determine densities, as has been done in studies with glassy polymers, because the *in situ* method for formation of copolymer requires the use of large quantities of material. For the present system, X-ray photoelectron spectroscopy (XPS) proved to be a useful analytical technique for investigating the interface, by monitoring the amount of nitrogen, which originated exclusively from the PA6. Using the ADCB test and XPS, we have investigated the kinetics of adhesion and the mechanisms of dissipation at the interface, and we will compare the results to those of glassy polymers and to theoretical models.

II. Experimental Section

1. Materials. The characteristics and properties of the polymeric materials used in this study are listed in Table 1. Commercial-grade polyamide-6 (PA6), obtained from BASF, had an average of one NH_2 end per chain. Commercial-grade polypropylene (PP), purchased from APPRYL, was 95% isotactic and had less than 1500 ppm of additives (mainly antioxidants). The functionalized polypropylene (PP_s) was obtained from ATOCHEM and had an average of one succinic anhydride group per chain. PP_s chains were diluted in pure PP at a weight fraction of 5%, giving a product denoted here as PP*. All polymeric materials were available as sheets with thicknesses of approximately 600 μm. Formic acid (Prolabo, 98-100%), trifluoroacetic anhydride (Aldrich), and dichloromethane (Prolabo or Merck) were used as received without further purification.

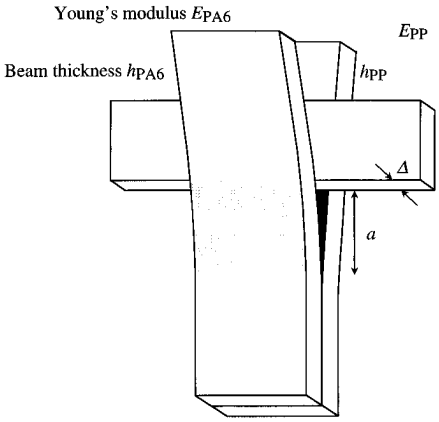

Figure 1. Schematic drawing of the geometry and parameters used in the ADCB test.

2. Preparation of Samples. Samples were made by clamping sheets of PA6 and PP* together in an airtight, Teflon-lined mold under slight pressure and then heating the molds in a temperature-controlled furnace between 185 and 220 °C. This temperature range is above the melting temperature of PP but below that of PA6. The amount of copolymer was changed by varying the temperature of the furnace and the length of time that the sample was left in the furnace. Molds were cooled down to room temperature in air at a measured cooling rate of approximately 4 °C/min. All samples were stored in an atmosphere of controlled humidity for at least 24 h prior to fracture, to give reproducible values for the Young's modulus of PA6. The thickness of one side (h) of a sample could be increased by adding an appropriate number of sheets. In general, total thicknesses for the samples ($h_{PP} + h_{PA6}$) were between 1.6 and 3.4 mm.

It is important to note that the conditions for forming the joints did not have an effect on certain bulk properties of the materials. Young's moduli and heats of fusion were measured for samples of PP and PA6 from joints that had been made over the entire range of experimental conditions, and their values and standard deviations are listed in Table 1. We included the heats of fusion rather than the degrees of crystallinity in Table 1, because of the wide variation in the literature values for the heats of fusion for pure crystals of PP and PA6. Given $\Delta H_{PP} = 209$ J/g and $\Delta H_{PA6} = 230$ J/g (the most current values),[10] we nevertheless obtain 43 and 30% for the degress of crystallinity in PP and PA6, respectively.

Due to the different thermal expansion coefficients ($\Delta\alpha$) of the two materials, adhered samples were slightly bent. From the mechanical constants of the two materials and the measured radius of curvature of a typical joint, the internal strain on the system was estimated to be 0.24%. This value gives $\Delta\alpha \approx 1.6 \times 10^{-5}$ K^{-1}, which is in agreement with data from the literature ($\alpha_{PP} = 6.8 \times 10^{-5}$ K^{-1}; $\alpha_{PA6} = (7-10) \times 10^{-5}$ K^{-1}).[11] For this $\Delta\alpha$, the bending energy is 1.5 J/m^2 for a 1.6 mm thick sample, which is less than the smallest fracture toughness measured in the present experiments.

3. Measurement of Energies of Adhesion. Fracture toughnesses were measured using an asymmetric double cantilever beam (ADCB) test, because it has been shown to be a reliable test for studying the fracture toughnesses of polymer−polymer interfaces.[6,8] Details of this method are shown in Figure 1: a blade of width Δ was inserted at the interface between the PP* and the PA6 and was pushed into the sample at a speed of 3 μm/s. We measured the energy of adhesion as a function of the speed between 0.3 and 300 μm/s and detected no influence over this four-decade range; we therefore assumed that the measured energy release rate at 3 μm/s is equal to G_c, the critical energy release rate at zero velocity.

Although the materials are semicrystalline, the PP side remained transparent enough at the experimental thicknesses to allow measurement of the crack length using a video camera. An image of the region ahead of the blade was recorded for every millimeter that the blade advanced. The

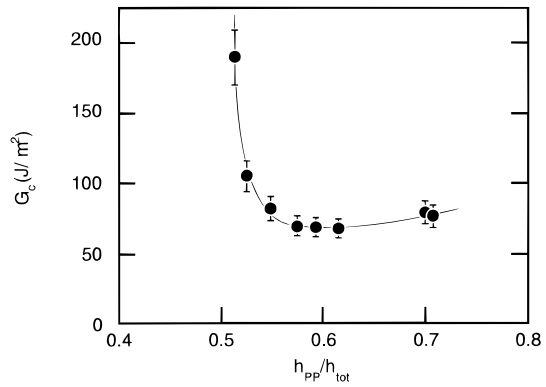

Figure 2. Effect of asymmetry on the measurement of G_c using the ADCB test. The *x*-axis presents the ratio of the thickness of the PP part of the sample to the total thickness (h_{PP}/h_{tot}). Equation 2 was used to calculate G_c. The line through the data is provided as a guide to the eye.

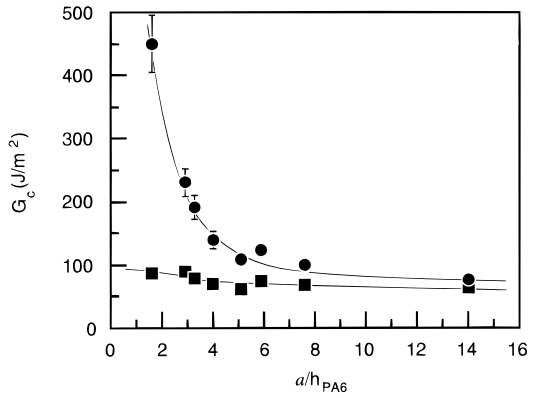

Figure 3. Plot of the strain energy release rate, G_c, against the ratio of the fracture distance to the thickness of the PA6 part of the sample (a/h_{PA6}). The circles were calculated using the simple-beam equation (eq 1), and the squares were calculated using the modified equation (eq 2). Lines through the data are provided as guides to the eye.

crack length and its standard error were then determined from at least 10 images. Although the deviation in measurements for a typical sample was around 5%, we estimated the accuracy of the measured energy of adhesion (G_c) to be around 10%, due to the accuracy of the physical constants and experimental parameters needed to determine G_c.

The ADCB test yields reliable values of G_c if two precautions are taken. First, the samples must be asymmetric—that is, $h_{PP}/h_{PA6} \neq 1$—because the different mechanical properties of the two polymers can induce various modes of fracture. Figure 2 illustrates the effect of asymmetry for samples that were prepared using the same experimental conditions, but whose relative thicknesses of the two sides were varied. It is known that varying the ratio of thicknesses changes the amount of K_{II} component in the fracture process[12] and that if the fracture tends to deviate into the more ductile material (PP in our case), the measured energy release rate can increase significantly, leading to substantial errors in the evaluation of G_c.[13] This effect is clearly observed in the present system: if the PP beam is not stiff enough relative to the PA6 beam (e.g., $h_{PP}/h_{tot} < 0.5$), the energy release rate is much larger than the observed minimum obtained for $h_{PP}/h_{tot} \approx 0.62$ (Figure 2). To minimize contributions of K_{II} components, all samples in this study were therefore made with the ratio h_{PP}/h_{tot} between 0.57 and 0.7.

Second, the critical energy release rate must be calculated in the proper limit. If the crack length ahead of the blade a is longer than $\sim 10h_{PA6}$, simple beam theory is a reasonable approximation and gives

$$G_c = \frac{3}{8}\frac{\Delta^2}{a^4}\frac{E_{PP}h_{PP}^3 E_{PA6}h_{PA6}^3}{E_{PP}h_{PP}^3 + E_{PA6}h_{PA6}^3} \quad (1)$$

In this equation, E_i and h_i denote the Young's modulus and the thickness of material i, respectively, and Δ is the thickness of the blade. This equation is, however, not applicable when $a < 10h_{PA6}$. Based on calculations by Kanninen,[14] whose central assumption was that the finite elasticity of the material ahead of the crack tip required correction factors for small crack lengths, we derived the following equation:

$$G_c = \frac{3}{8}\frac{\Delta^2}{a^4}\frac{E_{PP}h_{PP}^3 E_{PA6}h_{PA6}^3}{E_{PP}h_{PP}^3\alpha_{PA6}^2 + E_{PA6}h_{PA6}^3\alpha_{PP}^2} \quad (2)$$

where α_i, the correctional factor for material i, is

$$\alpha_i = \left(1 + 1.92\frac{h_i}{a} + 1.22\left(\frac{h_i}{a}\right)^2 + 0.39\left(\frac{h_i}{a}\right)^3\right)\Big/\left(1 + 0.64\frac{h_i}{a}\right) \quad (3)$$

Equation 2 is essentially the same as the one given in ref 6.

Figure 3 emphasizes the importance of using the modified equation: For various samples made under the same conditions, for which we therefore expected the same value of G_c, we tested different thicknesses of the blade in order to vary the crack length. The strain energy release rate was then estimated using eqs 1 and 2 (Figure 3). Clearly, the simple beam geometry assumed in eq 1 is only valid in our system for infinite crack lengths. With the modified equation, reasonable agreement is found among the calculated values of G_c for $4 < a/h_{PA6} < 14$. The assumptions used to derive eq 2, however, still lead to an overestimation of G_c for very short crack lengths, in agreement with numerical results.[15] To obtain reliable, reproducible values of G_c, we therefore controlled the thickness of the blade so that a/h_{PA6} was between 4 and 14, and we used eq 2 to calculate G_c.

4. X-ray Photoelectron Spectroscopy (XPS). X-ray photoelectron spectra were collected on a Surfaces Science SSX-100 spectrometer using a monochromatized Al $K_{\alpha 1}$ source ($h\nu = 1486.6$ eV). Survey scans between 0 and 1100 eV were initially taken on each sample to check for contamination of the interface.[16] On a clean area of the sample, spectra were collected for the 1s peaks of carbon, nitrogen, and oxygen near 285, 400, and 530 eV, respectively, using a spot size of 200 × 750 μm. The pass energy on the detector was 55 eV, which gives a window with a width of 7 eV for the detector. Binding energies were referenced to the peak due to hydrocarbon in the C 1s region at 284.8 eV. Spectra were fitted using 80% Gaussian/20% Lorentzian peak shapes and a Shirley background subtraction.[17] All spectra were collected at a take-off angle between the sample and the detector of 35° and with an electron flood gun of 9 eV to dissipate charge in the sample. Samples were analyzed within 10 days of preparation to minimize effects due to oxidation of the interface. The reproducibility in the measurements on a single sample was approximately ±10%. The spectrometer was also equipped with an argon ion sputtering gun that was operated at 3 kV with an emission current of 10 mA, which could be used to remove thin layers of polymer (for organic materials, the sputtering rate is around 5 nm/min).

5. Preparation of Samples for Determination of the Density of Copolymer. To determine the areal density of copolymer at the interface, it was necessary to remove one of the two bulk polymers and to evaluate quantitatively the remaining amount of that polymer. Since PA6 has a wider variety of chemical functionality than PP, we chose to analyze the PA6 chains grafted to the PP. The majority of the bulk PA6 was removed from an uncleaved section of a sample whose G_c had already been measured, using three baths of formic acid, a good solvent for PA6 that neither dissolves nor swells PP. Formic acid, however, does not completely remove the bulk PA6 (determined using infrared spectroscopy), because of hydrogen bonding between free chains near the interface and the grafted chains. Scheme 1 presents the procedure used to remove these remaining free chains of PA6: The PA6 was reacted with trifluoroacetic anhydride in the vapor phase (so as not to swell the PP significantly), which eliminated hydro-

Scheme 1

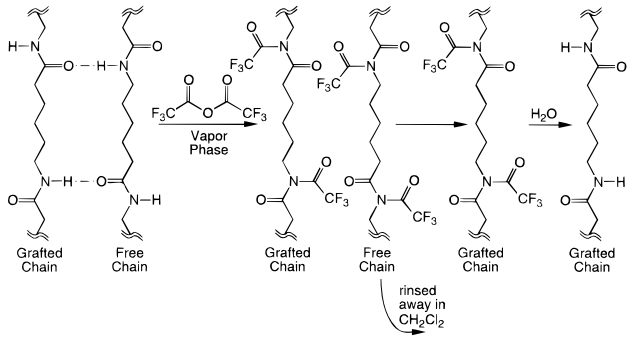

gen bond donors by forming the corresponding imide. After rinsing the samples with dichloromethane to remove the free chains, the trifluoroacetyl groups on the grafted chains were hydrolyzed with deionized water, which retransformed the grafted chains back to the original chemical formula of PA6.

6. Evaluation of the Density of Copolymers. Using samples prepared by the above procedure, we were able to determine the density of copolymer at the interface (Σ) from the intensity of the N1s peak in the XPS spectra. In evaluting Σ, we assumed that only the NH_2 groups reacted with the succinic anhydrides (which is confirmed by the results described in section III.1), that there was only one succinic anhydride group per chain, and that this succinic anhydride group was localized at the end of the chain.[18] The thickness of a PA6 layer (d) is related to the normalized N 1s counts (N/C) for the sample and the normalized counts for pure PA6 ($(N/C)_\infty$) in the following way:

$$\frac{(N/C)}{(N/C)_\infty} = 1 - \exp\left(-\frac{d}{\Lambda}\right) \tag{4}$$

The N 1s spectra were normalized relative to the carbon counts, which were effectively the same for pure samples of PP and pure samples of PA6, to ensure that fluctuations in the intensity of the X-ray source did not adversely affect the results. In eq 4, Λ is the escape length of the N 1s electrons including the take-off angle of the instrument and was estimated to be 19 Å using an experimentally determined relationship for escape lengths through hydrocarbon layers.[19] Because we have measured that one PA6 chain contains exactly one NH_2 end, we can relate Σ to d through eq 5,

$$\Sigma = N_a \rho d / M_n \tag{5}$$

where N_a is Avogadro's number, ρ is the mass density of PA6, and M_n is the number-average molecular weight of PA6. Combining eqs 4 and 5 directly relates the measured XPS intensity to the average areal density of copolymer (eq 6).

$$\Sigma = -(N_a \rho / M_n)\Lambda \ln\left(1 - \frac{(N/C)}{(N/C)_\infty}\right) \tag{6}$$

III. Results

1. Chemical Nature of the Copolymer. In order to prove that the presence of copolymer was the dominant factor in the adhesion between PP* and PA6, we attempted to make a joint between pure PP and PA6. After having been heated in the mold above the melt temperature of PP, the sample completely delaminated before the interfacial energy could be measured, implying an interfacial strength lower than 1.5 J/m^2. This result is expected, because the Flory parameter between PP and PA6 is greater than unity, given their solubility parameters ($\delta_{PP} = 18.8$ J$^{1/2}$/m$^{3/2}$, $\delta_{PA6} = 27.8$ J$^{1/2}$/m$^{3/2}$).[11] This situation contrasts that for glassy polymers where natural adhesion was low, but measurable.

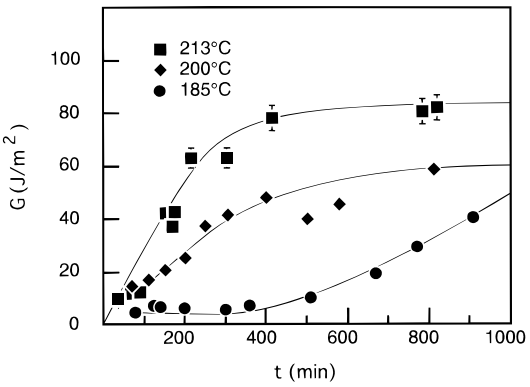

Figure 4. Energy of adhesion, G_c, as a function of the time in the mold for 185 (circles), 200 (diamonds), and 213 °C (squares). The absolute time scale is based on the amount of time after the PP had melted. Lines through the data are provided as guides to the eye.

Scheme 2

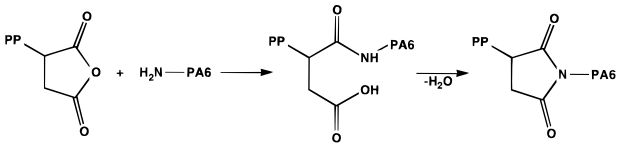

To show that the PA6 was reacting only through its NH_2 end groups,[20] we made a joint between PP* and PA6 that nominally had only carboxylic acids as end groups (di-COOH PA6).[21] The energy of adhesion G_c was 30 times smaller for this joint than for a joint formed under similar conditions with normal PA6. The residual adhesion was due to a small concentration of NH_2 groups remaining in the di-COOH PA6: slides of di-COOH PA6 turned light blue after reaction with a solution of ninhydrin in hot butanol.[22] We were able to reduce the amount of NH_2 groups by reacting a slide of di-COOH PA6 with succinic anhydride in boiling 2-propanol. After 3 h of reaction, the energy of adhesion went down again by a factor of 2.

These two results show that the copolymer is the dominant component for bonding a joint between PP* and PA6 and that it is formed *in situ* by the formation of a covalent bond between a PP_s chain and an NH_2 end of PA6. Reaction does not occur between succinic anhydride (or the corresponding diacid) and the amides of PA6. Scheme 2 presents the chemical reactions and the expected products.

2. Energy of Adhesion as a Function of Time and Temperature. To be able to control the density of copolymer at the interface between the two polymers, we have investigated the energy of adhesion (G_c) as a function of the temperature and the time of joining between the samples. We deliberately chose relatively low operating temperatures to allow variation in G_c over two orders of magnitude (1−100 J/m^2). Above the melt temperatures of both materials ($T > 220$ °C), we observed a rapid increase in G_c during the first few minutes, which did not allow for controlled variation in G_c. By making joints above the melt temperature of PP but below that of PA6 ($185 \le T \le 220$ °C), it was possible to spread the whole process in time.

Figure 4 presents G_c as a function of the time of reaction at three temperatures for PP_s with $M_n = 23\,000$ doped in PP at a weight fraction of 5%. At 213 °C, the energy of adhesion saturated near 80 J/m^2 after 400 min, suggesting that the interface had reached a level of saturation. Lowering the temperature to 200 °C

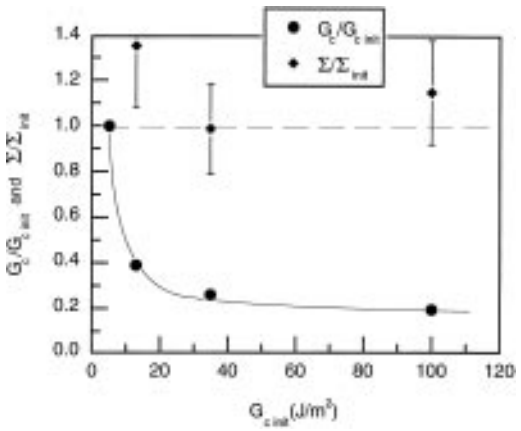

Figure 5. Results from rewelding experiments. Circles: ratio of final energy of adhesion to initial energy of adhesion ($G_c/G_{c\,init}$) plotted against the initial energy of adhesion ($G_{c\,init}$). Diamonds: ratio of the measured final areal density of copolymer to the estimated initial areal density of copolymer (Σ/Σ_{init}) against the initial energy of adhesion. The initial areal densities of copolymer were estimated from the relationship between G_c and Σ shown Figure 9.

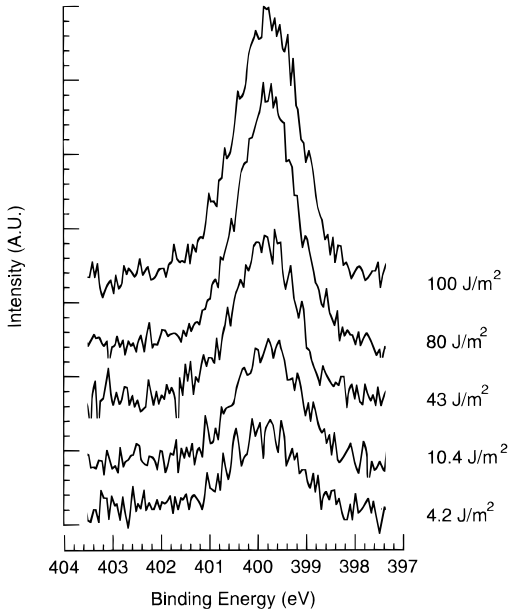

Figure 6. Representative X-ray photoelectron spectra in the nitrogen 1s region for samples made across the entire range of energies of adhesion. Energies of adhesion are given next to their respective peaks. The signals have been normalized by the carbon counts for the sample, as we have found that the carbon counts do not vary significantly between pure samples of PP and pure samples of PA6.

slowed the rate of increase of G_c and reduced its value of saturation. Decreasing the temperature further to 185 °C leads to even more dramatic effects: the interfacial toughness rapidly increased to 6 J/m^2, but remained at this value for approximately 400 min, after which the rate of growth was slightly less than that at 200 °C. The origin of this plateau is currently not understood, but may be due to annealing of the PA6 at this temperature.

3. Analysis of Cleaved Surfaces. We investigated fractured joints with scanning electron microscopy (SEM) and X-ray photoelectron spectroscopy (XPS) to elucidate the mechanism by which the stored energy was dissipated during fracture. Results from SEM showed that the roughness of the PP side of the joint increased with increasing energy of adhesion. On the micron scale, the roughness appeared to be due to broken fibrils. On the PA6 side of the joint, however, the roughness of the surfaces did not change observably. From these results, we concluded that plastic deformation occurred on the PP* side.

We then investigated these same joints with XPS to understand more precisely the path of the crack at the interface. The key elemental difference between the two polymers is the presence of nitrogen in the PA6. Over a wide range of G_c, we found no nitrogen on the PP* side of the fracture. The nitrogen signal on the PA6 side, however, decreased relative to that of pure PA6, implying the presence of PP on this side. After rinsing the PA6 side in boiling xylenes, a good solvent of PP, the nitrogen signal increased, although not to the level of pure PA6, suggesting the presence of grafted PP.

Since these previous results strongly suggest that grafted PP remains on the PA6 side after cleavage, we attempted to form joints between PA6 sides after cleavage and pure PP (i.e., containing no PP$_s$). In these experiments, we took samples whose energies of adhesion were known, gently delaminated them, put the PA6 side in a mold with pure PP, and heated the sample under similar conditions used to form the original joint.[23] The circles in Figure 5 present the ratio of the final G_c to the initial energy of adhesion, $G_{c\,init}$, plotted against $G_{c\,init}$. These data clearly show that, at energies of adhesion above 10 J/m^2, the recovered energies of adhesion were significantly lower than the initial values, implying either a lower concentration of copolymer chains at the interface after initial cleavage or chain breakage of the PP chains during cleavage. To be able to differentiate between these two possibilities, we needed to determine the areal density of copolymer chains before and after the initial cleavage.

Since the PA6 part of the copolymer chain is not altered during fracture, we were able to measure the density of copolymer (Σ) after rewelding by evaluating the amount of PA6. (See the Experimental Section and the following section for more details on the determination of Σ.) The diamonds in Figure 5 present the ratio of the density after cleavage to the estimated original density, Σ_{init}, evaluated from Figure 9. This ratio was approximately 1 over the whole range of G_c, implying that *the number* of copolymer chains was the same before and after fracture. From these results, we can infer that the PP parts of the grafted chains are broken during initial cleavage, because the areal density of copolymer did not change, but the energy of adhesion decreased after rewelding. (We should note for the sample whose $G_{c\,init}$ was 5 J/m^2, we cannot distinguish between possible mechanisms of failure, because it is possible that the PP chains broke near their ends but that this change in length did not affect G_c.) These results strongly suggest that ultimate failure of PP−PA6 joints held together by diblock copolymers occurs by chain cleavage of the PP.

4. Determination of Areal Density of Copolymer at the Interface. One of the main goals of the present work was to determine the relationship between the energy of adhesion and the density of copolymer chains at the interface, Σ. We found XPS to be a reliable technique for determining Σ by measuring the amount of PA6 that remained on the PP side of joint after the bulk PA6 had been completely washed away (see the Experimental Section and Scheme 1 for details). Figure 6 presents representative XPS spectra in the nitrogen 1s region for samples with various values of G_c. From

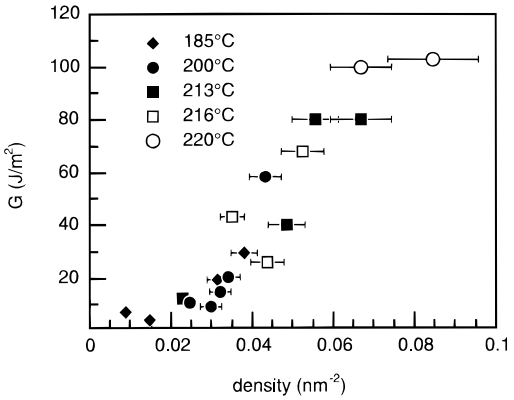

Figure 7. Energy of adhesion, G_c, as a function of the areal density of copolymers at the interface, Σ, at various temperatures of formation. Energies of adhesion were determined using the ADCB test. Areal densities of copolymers were determined using XPS. Error bars were determined by a propagation of the precision of the XPS data.

these data, it is important to note first that for each sample there is only one peak for nitrogen at 399.8 eV (relative to the carbon 1s peak for hydrocarbon at 284.8 eV), in good agreement with the literature value for amides.[24] These data also clearly show that the amount of PA6 increases with G_c. In order to prove that the nitrogen 1s signal was due to PA6 at the interface, we sputtered a sample with argon ions. After 1 min of sputtering, no nitrogen could be detected in the sample, implying that the original nitrogen 1s signal came exclusively from material on the surface of the sample.

The results of the ADCB test can be combined with the XPS surface analysis to give the strength of the interface G_c as a function of the areal density of copolymer chains Σ (Figure 7). It is immediately clear from these data that the presence of grafted chains has a strong influence on the measured G_c over the whole range of investigated areal densities. G_c increases monotonically with Σ regardless of the annealing time of the interface, implying that the reinforcement effect is not due to a modification of the bulk properties of one of the polymers during the annealing process, but rather depends uniquely on the areal density of copolymer chains formed at the interface.

IV. Discussion

1. Origin of the Kinetics of Grafting. To calculate diffusion coefficients from the data in Figure 4, we needed to assume that the rate of reaction was significantly large so as not to be the cause of the observed rate of increase of the energy of adhesion. The consistency of this assumption is demonstrated in this paragraph: although the ultimate product we expect at the interface is the imide formed between a succinic anhydride on the PP_s and an NH_2 end of the PA6, the important step is the formation of the succinamidic acid (the first step in Scheme 2), since this step creates the bond at the interface. In water, aliphatic succinamidic acids are formed with rate constants on the order of 10^3 M^{-1} s^{-1} at room temperature.[25] Since the rates of these reactions are not significantly affected by the polarity of the solvent,[26] we used the activation energy and rate constant for the reaction between 2-fluoroethylamine and maleic anhydride in water ($E_a = 11$ kcal/mol and $k = 10^4$ M^{-1} s^{-1} at 25 °C)[27,28] and the concentrations of amine and succinic acid in our system to estimate the rate of reaction in our system.[29] From these values, we determined a rate of formation of copolymer of approximately 10^3 M/s at 200 °C. From this value, we can infer that the observed rates are primarily due to the diffusion of PP_s to the PP−PA6 interface.

Table 2. Coefficients of Diffusion for PP_s in Bulk PP

temp, °C	$G_{c\infty}$,[a] J m^{-2}	(dG_c/dt),[a] J m^{-2} s^{-1}	D, cm^2 s^{-1}
213	80	5.0×10^{-3}	15.8×10^{-12}
200	60	2.1×10^{-3}	8.9×10^{-12}
185	60	1.3×10^{-3}	5.6×10^{-12}

[a] Estimated from Figure 4.

As the interface becomes saturated with copolymer chains, the rate slows down. Before the interface is saturated, at 200 and 213 °C, the value of (dG_c/dt) at the origin can give the unpertubed coefficient of diffusion. We believe that the lag time that appeared at 185 °C is due to partial crystallization of PA6 at that annealing temperature, although we have no direct evidence at present. After 400 min, normal mobility is recovered. At this temperature, we determined the coefficient of diffusion by taking (dG_c/dt) in the increasing part of Figure 4. Since the chemical reaction is very fast, we can link the density of grafting Σ to the time t by a standard diffusion equation[30]

$$\Sigma = 2c_0(\Sigma_\infty a^2)\left(\frac{Dt}{\pi}\right)^{1/2} \tag{7}$$

where D is the diffusion constant, c_0 is the volume concentration of succinic anhydride (10^{24} m^{-3}), a^2 is the surface area of a monomer (17.6 Å^2, which was calculated by taking the two-thirds root of the volume per monomer), and Σ_∞ is the density at saturation. Values of Σ were determined from values of G_c using the relationship in Figure 9. D can then be determined by

$$D = \frac{\mathrm{d}G_c/\mathrm{d}t}{G_{c\infty}\left(\frac{2c_0a^2}{\pi^{1/2}}\right)^2} \tag{8}$$

where (dG_c/dt) is the slope of Figure 4 at the origin (used for 200 and 213 °C; the case of 185 °C is described above) and $G_{c\infty}$ is the energy of adhesion at saturation determined from Figure 4. Table 2 summarizes assumed values for (dG_c/dt) and $G_{c\infty}$ at various temperatures and the calculated values of D.

The estimations are in good agreement with previous results measured for polyethylene (PE):[31] for PE with the same polymerization as PP_s, we calculate D to be around 50×10^{-12} cm^2 s^{-1} at 235 °C from the data in ref 31. As one can see in Figure 8, these data points are consistent with a law given by

$$D = D_\infty \exp\left(\frac{-E_a}{R(T - T_g)}\right) \tag{9}$$

with an activation energy $E_a = 12 \pm 2$ kJ mol^{-1}. D_∞ is difficult to determine accurately with only these three data points; nevertheless, its order of magnitude is 10^{-8} cm^2 s^{-1}.

2. Relationship between *G* and Σ. Studies on the adhesion between incompatible glassy polymers reinforced with diblock copolymers have yielded two general relationships between the energy of adhesion and the areal density of copolymer chains at the interface. In the regions of simple chain pullout or chain scission, the energy of adhesion scales linearly with the amount of copolymer; when one of the polymers crazes during

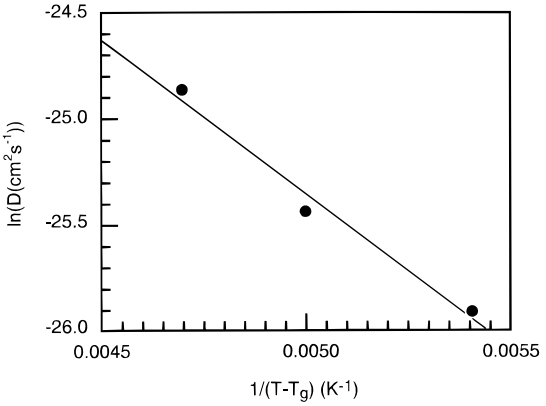

Figure 8. Arrhenius plot for the coefficients of diffusion given in Table 2. The line represents a best fit to data.

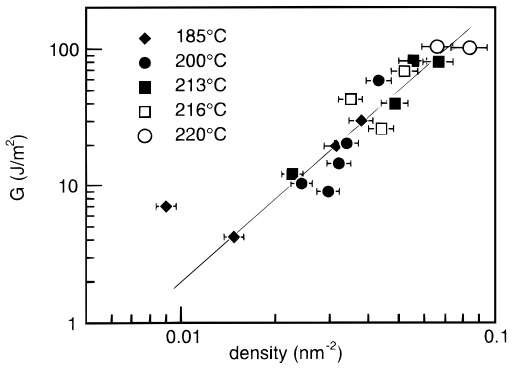

Figure 9. Relationship between the energy of adhesion and the areal density of copolymers plotted on a log−log scale to show the square-law behavior. The line is a best fit to all of these data and gives a slope of 2.03 ± 0.18. The explanation for the error bars is given in the caption to Figure 7.

separation, the energy of adhesion increases with the square of the density. From Figure 7, it is obvious that the relationship between G and Σ is not linear; the exact behavior of our system and the number of regimes are, however, not obvious. Figure 9 shows the data from Figure 7 in a log−log plot. Fitting the entire set of data yields an exponent of 2.03 ± 0.18. Given the order of magnitude of the values of G_c and the fibrillation that was observed after cleavage of strongly adhered samples, one might have expected a relationship similar to that observed for glassy polymers in the crazing regime. Several interesting observations come from this plot. First, the conditions for forming the samples do not affect the relation between G and Σ. Second, there is only one obvious regime, suggesting that the mechanism of dissipation is similar for all values of Σ.

To explain the square-law dependence for glassy polymers, Brown developed a model based on the microscopic parameters of the interface.[8] As a starting point, he used Dugdale's description of the relationship between the size of the plastic zone[32] and the applied stress; the Dugdale model yields a general shape for a plastic zone, which has been verified for crazing in glassy polymers.[33] For a linearly elastic and perfectly plastic material, the energy of adhesion is related to the final width of the plastic zone at the crack tip (h_f) through

$$G_c = \sigma_y h_f(1 - 1/\lambda) \tag{10}$$

where σ_y is the yield stress of the material and λ is the extension ratio of a craze fibril.[33] Because eq 10 is not explicitly defined in terms of the properties of the materials, Brown sought to relate the final width of the plastic zone, which is macroscopic, to the microscopic parameters that control it, and consequently the energy of adhesion. His main assumption was to consider the craze as an elastically anisotropic continuum with a small but finite shear modulus in the direction parallel to the fibrils. This nonzero shear modulus, justified physically by the existence of cross-tie fibrils, causes a "small-scale" stress concentration within the crazed polymer and is therefore ultimately responsible for propagation of the crack. This increase in stress is localized over a length D, for which Brown used the diameter of the fibrils. Since D is significantly smaller than the length of the crack, most of the plastic zone is still drawn at the constant stress σ_y, which validates the use of eq 10 for determining G_c. In the region of stress concentration, failure occurs when the stress near the crack tip reaches the stress needed to break chemical bonds in the backbone of the polymer (σ_f). Using fracture mechanics, Brown derived the following relationship for the microscopic stress as a function of the other parameters of the interface:

$$\frac{\sigma_f}{\sigma_y} \sim \left(\frac{h_f}{D}\right)^{1/2} \tag{11}$$

Brown then used

$$\sigma_f = \Sigma f_b \tag{12}$$

as a reasonable estimate of σ_f by considering that the ultimate stress that the material could bear was the force needed to break a chemical bond in the chain, f_b, multiplied by the areal density of chains. Combining eqs 10−12 gives the relationship $G \sim \Sigma^2$. Specifically, the detailed calculation yields

$$G_c = \frac{\Sigma^2 f_b^{\,2}(2\pi D)}{\sigma_y}\left(\frac{S_{22}}{S_{12}}\right)^{1/2}(1 - 1/\lambda) \tag{13}$$

where S_{22} and S_{12} are the tensile and shear compliances of the crazed material, respectively.

Because the above model was derived for glassy polymers, it is not obvious that the specific details of its framework can be applied to semicrystalline polymers. First, it is important to consider the manner by which PP yields during cleavage. Although PP does craze below its glass transition temperature ($T_g \approx 4$ °C for our PP), thin films of PP exhibit shear bands when deformed under conditions of plane stress above T_g.[34,35] The experimental conditions of the ADCB test (i.e., the geometry of cleavage and the width of the samples), however, enforce the condition of plane strain in the sample. Coupled with the incompressibility of the polymers, plane strain can lead to cavitation, analogous to fibrillar shear at room temperature. The size of fibrils in semicrystalline polymers is often on the micron scale, compared with 10 nm for glassy polymers.[34]

The main consequence of the size of these fibrils is that they may not fit with Brown's model, which overestimates the results relative to a discrete modeling of the fibrillar structure proposed by Sha et al. in the limit of thin plastic zones (i.e., small energies of adhesion).[36] The continuum theory of Brown is, however, found to be in good agreement with the discrete model when $[\sigma_y/\Sigma f_b]^2 < 1$.[36] Using values for PP ($\sigma_y \cong 27$ MPa and $f_b \cong 2 \times 10^{-9}$ N) in this relationship, we calculate $\Sigma = 0.0135$ nm^{-2} as the lower limit at which the PP*/

PA6 system will follow the continuum theory; this value of Σ is also approximately the lower limit of observed areal densities measured in the present experiments. The relative ductility of PP, therefore, explains why the square law is well verified in the present case.

Second, we must emphasize that the assumption of stress concentration will always yield a Σ^2 dependence for G_c, regardless of the fibrillar structure of the plastic zone. As the observed Σ^2 dependence for PP/PA6 assemblies suggests the existence of a structure able to support large stresses at the crack tip, and since we have shown that failure of the plastic zone occurs by chain scission (section III.3), it is possible to apply eq 13 to PP/PA6 assemblies in order to determine the extension of the stress concentration D. This estimation of D yields 10 nm, because the other parameters of eq 13 are of the same order of magnitude as those for glassy polymers. Since the size of the fibrils in semicrystalline polymers is *much larger* than this calculated length, the stress concentration at failure may be occurring on the macromolecular scale rather than over the whole width of the fibril.

The similarity between this semicrystalline system and the glassy cases could be due to a unique aspect of the morphological behavior of PP. By quickly quenching the melt, PP forms a disordered phase, or "smectic" phase,[37] which can be described as a laterally disordered packing of parallel 3_1 helixes of PP chains with high order in the direction of the helix axis.[38] This phase is also formed when PP in the α-phase is highly drawn.[39] If this morphological change occurs during formation of fibrils in the plastic zone, it could explain the similarities in the fracture behaviors of glassy systems and PP, and, consequently, why the presence of spherulites in the PP appears to have no effect on the energy of adhesion.

Since we know that the crystal organization has a deep effect on the yield stress, we expect to see a change in the adhesive properties if we change the crystal organization close to the interface. As a matter of fact, we have checked by wide-angle X-ray scattering that all the present samples exhibit the same crystal structure (i.e., the α-phase). By modifying the experimental procedure of making the joints, we could actually change the crystal organization and therefore the adhesive behavior of the PP*/PA6 system. This topic will be addressed in a forthcoming paper.

V. Summary

The results from the present experiments have begun to detail several aspects of the formation and toughness of reinforced interfaces between PP and PA6. The behavior during formation is relatively simple to understand: at the present concentration of PP_s, formation of joints between PA6 and PP* is limited by the diffusion of these chains to the interface between the two materials. This result allows one to calculate the amount of copolymer formed at a specific temperature and a specific time, thus providing a means of forming materials with certain values of interfacial toughness.

The mechanism and the mechanics of failure are, however, more complicated. We have shown that during fracture, dissipation takes place in the PP, the more ductile of the two materials, by formation of a plastic zone. This plastic zone ultimately fails by chain scission of the PP blocks of the copolymers, which implies that molecular weight of the PP block should have no effect on the toughness of the interface, as long as the mechanism of dissipation remains the same.[8]

Despite the complex morpology of the materials, the relationship between the energy of adhesion and the areal density of copolymer is very similar to that of glassy polymers. The present system follows the general relation predicted by Brown, even at low areal densities, because of the ductility of the PP,[12,36] implying that the stresses are concentrated at the tip of the crack during failure. The only apparent divergence between the present system and Brown's model for glassy polymers is that the size of the fibrils in PP is *much larger* than the calculated region of concentration of stresses. We might conclude that although the final width of the plastic zone (h_f, which lies on the micrometer scale) is the visible parameter controlling the energy of adhesion, the strength of an interface depends stronly on structural interactions of the scale of 10 nm, which is closer to a macromolecular length, suggesting that the local organization of the chains is ultimately responsible for the efficiency of the dissipation and the toughness of the interface.

Acknowledgment. We are strongly indebted to ELF ATOCHEM for providing the materials used in this study and for financial support, and we thank Christian Quet (ELF ATOCHEM, Lacq) for the XPS data. We have benefited from particularly fruitful discussions with H. R. Brown during his stay at the Collège de France from April to June, 1994, and with C. J. G. Plummer. J.P.F. would like to thank the French Ministry of Education for postdoctoral support and also Professor Robert Carey (University of Georgia) for advice concerning the chemistry of amides.

References and Notes

(1) Fayt, R.; Jérôme, R.; Teyssié, Ph. *J. Polym. Sci., Polym. Phys. Ed.* **1989**, *27*, 775.
(2) Leibler, L. *Makromol. Chem., Macromol. Symp.* **1988**, *16*, 1.
(3) Dai, C.-A.; Dair, B. J.; Dai, K. H.; Ober, C. K.; Kramer, E. J.; Hui, C.-Y.; Jelinski, L. W. *Phys. Rev. Lett.* **1994**, *73*, 2472.
(4) Kramer, E. J.; Norton, L. J.; Dai, C.-A.; Sha, Y.; Hui, C.-Y. *Faraday Discuss.* **1994**, *98*, in press.
(5) Washiyama, J.; Kramer, E. J.; Creton, C. F.; Hui, C.-Y. *Macromolecules* **1994**, *27*, 2019.
(6) Creton, C. F.; Kramer, E. J.; Hui, C.-Y.; Brown, H. R. *Macromolecules* **1992**, *25*, 3075.
(7) Washiyama, J.; Creton, C. F.; Kramer, E. J. *Macromolecules* **1992**, *25*, 4571.
(8) Brown, H. R. *Macromolecules* **1991**, *24*, 2752.
(9) Hobbs, S. Y.; Bopp, R. C.; Watkins, V. H. *Polym. Eng. Sci.* **1983**, *23*, 380.
(10) Wunderlich, B. *Macromolecular Physics*; Academic: New York, 1980; Vol. 3, pp 48−57.
(11) Brandrup, J.; Immergut, E. H. *Polymer Handbook*, 2nd ed.; John Wiley and Sons: New York, 1975.
(12) Brown, H. R. *J. Mater. Sci.* **1990**, *25*, 2791.
(13) For a system of polystyrene (PS) and poly(2-vinylpyridine) (PVP), oblique crazes formed from the interface ahead of the crack tip in the PS when K_{II} was nonzero. When K_{II} was greater than zero, the crazes were formed at 45° relative to the direction of the fracture. These crazes contributed greatly in the evaluation of G_c. When K_{II} was less than zero, the direction of the oblique crazes was 135°, but the crazes did not grow significantly, because of the unfavorable stress field. These crazes, therefore, did not contribute significantly to the measured fracture toughness: Xiao, F.; Hui, C.-Y.; Washiyama, J.; Kramer, E. J. *Macromolecules* **1994**, *27*, 4382.
(14) Kanninen, M. F. *Int. J. Frac.* **1973**, *9*, 83.
(15) Xiao, F.; Hui, C.-H.; Kramer, E. J. *J. Mater. Sci.* **1993**, *28*, 5620.
(16) The most common element identified with contamination of the surface was silicon, which probably originated from silicone grease used in various steps of the cleaning.
(17) Shirley, D. A. *Phys. Rev. B* **1972**, *5*, 4709.
(18) De Roover, B.; Sclavons, M.; Carlier, V.; Devaux, J.; Legras, R.; Momtaz, A. *J. Polym. Sci., Polym. Chem. Ed.* **1995**, *33*, 829.

(19) Laibinis, P. E.; Bain, C. D.; Whitesides, G. M. *J. Phys. Chem.* **1991**, *95*, 7017.
(20) A recent study had addressed the relative reactivities of amine/anhydride and amide/anhydride reactions for polyamides and has concluded that the reactivity of the amides is very small compared to that of the amines: Maréchal, P.; Coppens, G.; Legras, R.; Dekoninck, J.-M. *J. Polym. Sci., Polym. Chem. Ed.* **1995**, *33*, 757.
(21) PA6 that nominally had carboxylic acids at each end was prepared by ATOCHEM and had the same melt flow index as that of the normal PA6 obtained from BASF.
(22) Roberts, R. M.; Gilbert, J. C.; Rodewald, L. B.; Wingrove, A. S. *Modern Experimental Organic Chemistry*, 4th ed.; Saunders College: Philadelphia, 1985; p 661.
(23) Note that it was not possible to reweld PA6 on the PP* side of the joint due to the presence of PP_s.
(24) See, for example: Beamsom, G.; Briggs, D. *High Resolution XPS of Organic Polymers*; John Wiley and Sons: Chichester, 1992; p 198.
(25) Pitman, I. H.; Uekama, K.; Higuchi, T.; Hall, W. E. *J. Am. Chem. Soc.* **1972**, *94*, 8147. Hall, W. E.; Higuchi, T.; Pitman, I. H.; Uekama, K. *J. Am. Chem. Soc.* **1972**, *94*, 8153.
(26) Loucheux, M.-H.; Banderet, A. *Bull. Soc. Chim. Fr.* **1961**, 2242.
(27) Kluger, R.; Hunt, J. C. *J. Am. Chem. Soc.* **1984**, *106*, 5667.
(28) Because few activation energies for reactions between amines and cyclic anhydrides are available, we used the present values as a best approximation.
(29) $[NH_2] \approx 6 \times 10^{-2}$ M in PA6 with $M_n = 17\ 000$; [succinic anhydride] $\approx 2 \times 10^{-3}$ M in PP*.
(30) Crank, J. *The Mathematics of Diffusion*, 2nd ed.; Clarendon: Oxford, 1975.
(31) Klein, J. *Nature (London)* **1978**, *271*, 143.
(32) Dugdale, D. S. *J. Mech. Phys. Solids* **1960**, *8*, 100.
(33) Döll, W.; Könczöl, L. *Adv. Polym. Sci.* **1990**, *91/92*, 137 and references therein.
(34) Jang, B. Z.; Uhlmann, D. R.; Vander Sande, J. B. *Polym. Eng. Sci.* **1985**, *25*, 98.
(35) Olf, H. G.; Peterlin, A. *J. Polym. Sci., Polym. Phys. Ed.* **1974**, *12*, 2209.
(36) Sha, Y.; Hui, C.-H.; Ruina, A.; Kramer, E. J. *Macromolecules* **1995**, *28*, 2450.
(37) Natta, G.; Peraldo, M.; Corradini, P. *Rend. Acc. Naz. Lincei* **1959**, *26*, 14.
(38) Balta-Calleja, F. J.; Peterlin, A. *J. Polym. Sci., Part A-2* **1972**, *10*, 1749.
(39) Kammer, H. W.; Kummerloewe, C.; Greco, R.; Mancarella, C.; Martuscelli, E. *Polymer* **1988**, *29*, 963.

MA9509422